Cement and Concrete Research 40 (2010) 1451–1458

Contents lists available at ScienceDirect

Cement and Concrete Research

journal homepage: http://ees.elsevier.com/CEMCON/default.asp

Potentiostatic transient technique, a simple approach to estimate the corrosion current density and Stern–Geary constant of reinforcing steel in concrete

A. Poursaee

School of Civil Engineering, Purdue University, West Lafayette, IN, 47907, USA

ARTICLE INFO

Article history:
Received 26 January 2010
Accepted 19 April 2010

Keywords:
Corrosion (C)
Electrochemical properties (C)
Stern–Geary constant

ABSTRACT

The linear polarization resistance (LPR) method, introduced by Stern and Geary, is widely used in determining corrosion rates of steel bars in concrete or synthetic pore solution. The major limitation of this method is that the value of the Tafel slopes, and consequently the Stern–Geary constant (B), is necessary for accurate calculation of the corrosion rate. This paper proposes a simple method for determining the corrosion current density and the Stern–Geary constant, using the results of the potentiostatic transient technique. The effect of the Stern–Geary constant on the corrosion rate of steel bar in concrete is also discussed. Results of this study show that potentiostatic transient method can be used successfully to determine the corrosion rate of steel bars in concrete without using the pre-assumed value of *B*.

1. Introduction and background

Linear polarization resistance (LPR) measurements are performed by applying a potential usually in the range of ±20 mV about the corrosion potential (E_{corr}), either as a constant pulse (potentiostatic) or a potential sweep (potentiodynamic) and measuring the current response. In addition, a current pulse (galvanostatic) or a current sweep (galvanodynamic) can be applied and to measure the potential response. The relationship between potential and current in this potential range is approximately linear, as shown schematically in Fig. 1. Polarization resistance, which represents the resistance of the specimen to oxidation while an external potential is applied, can be determined by calculating the slope of this linear region:

$$R_p = \frac{\Delta E}{\Delta I} \tag{1}$$

where R_p is the polarization resistance (Ω), ΔE is change in potential (V) and ΔI is change in current (A). The Stern–Geary equation relates corrosion current to R_p [1]:

$$I_{corr} = \frac{B}{R_p} \tag{2}$$

where B is the Stern–Geary constant and can be determined using anodic (β_a) and cathode (β_c) Tafel slopes:

$$B = \frac{\beta_a \beta_c}{2.3(\beta_a + \beta_c)}. \tag{3}$$

The value of B for steel bars in concrete is typically considered as 26 mV for active and 52 mV for passive corrosion [2,3]. These values have been used in calculations of corrosion rates for many years. It should be noted that, originally, these values were validated for steel in saturated $Ca(OH)_2$ solution [2] which is basically a rough simplification of the actual environment found inside the concrete. In many studies and commercial however, the original Stern–Geary equation is applied without questioning the adequacy of the assumed constants and the polarization conditions used. In practice, the corrosion activity of steel in concrete is more complicated than that in saturated $Ca(OH)_2$ or even simulated pore solution and the suitability of the proposed B values for the complex corrosion mechanism of steel in concrete has not been fully addressed [4–6]. In the theoretical analysis by Song [6] it was shown that the values of B for steel in concrete can be from 8 mV to ∞, based on different conditions and corrosion activities. Based on the work of Alonso et al. [7], the value of B would be 125 and 191 mV for damp concrete and concrete at the ambient humidity, respectively. From the investigation of the polarization curves of steel in concrete specimens containing various percentages of sodium chloride performed by Locke and Siman [8], the range of 75 to 278 mV can be calculated for B.

Therefore, it can be concluded that the value of B is not constant and it changes based on the anodic and cathodic reactions and using the same value for all measurements and environments may cause errors in the calculations. As a result, it is important to determine the value of B for each measurement or to determine the corrosion rate without using B.

A common method to determine the Tafel slopes is using anodic and cathodic potentiodynamic polarization curves. Using the slope of the linear region of each curve, β_a and β_c can be determined. While a cathodic Tafel slope can be measured relatively easily using the

E-mail address: poursaee@purdue.edu.

0008-8846/$ – see front matter © 2010 Elsevier Ltd. All rights reserved.
doi:10.1016/j.cemconres.2010.04.006

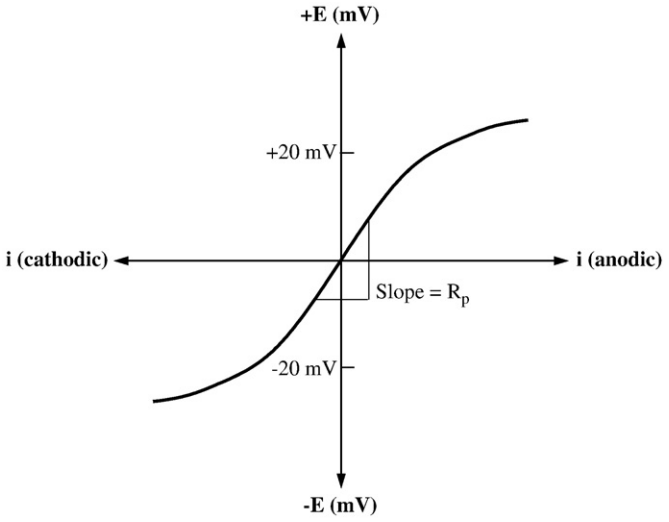

Fig. 1. Schematic illustration of linear polarization curve and polarization resistance (R_p).

cathodic polarization curves, oftentimes, there is no reasonable linearity of the anodic parts of the polarization curves. The reason could be due to rapid anodic dissolution, which can cause undesirable disturbance of the system before the anodic polarization curve is complete [9]. When that is the case, in order to determine the value of β_a the anodic data can be derived from the linear portion of the cathodic curve [10]. Fig. 2 is a schematic illustration of this technique. The measured values of current which are given on the polarization curves are in fact the net values. This means that each point on the cathodic part of the curve is the difference between cathodic and anodic currents and each point on the anodic part of the curve is the difference between anodic and cathodic currents:

$$i_{\text{net, a}} = i_c - i_a \tag{4}$$

$$i_{\text{net, c}} = i_a - i_c \tag{5}$$

where $i_{\text{net, a}}$ is the current on the anodic curve, $i_{\text{net, c}}$ is the current on the cathodic curve, i_c is the cathodic current and i_a is the anodic current

The anodic current density (i_a) can be calculated as:

$$i_a = i_{\text{net, c}} - i_c. \tag{6}$$

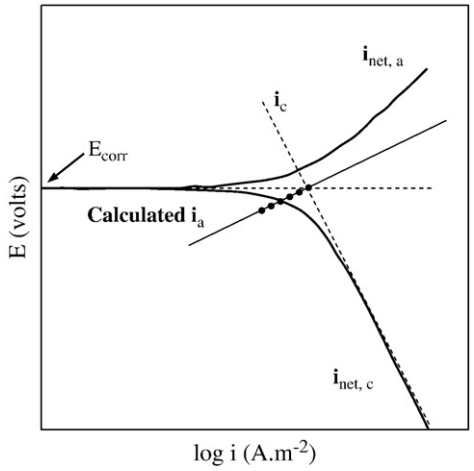

Fig. 2. Illustration of the method, used to determine anodic polarization curve from cathodic curve (adapted from [10]).

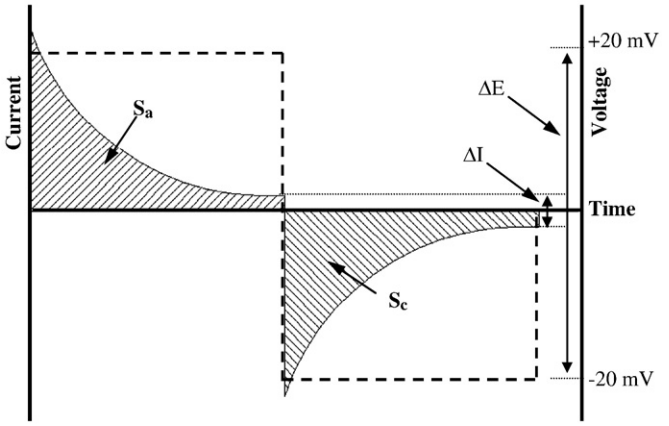

Fig. 3. Applied potential and current response during LPR measurement.

In the potential region near corrosion potential, the extrapolated Tafel line gives i_c, and the measured values (data points) give i_{net}. By using this method for a number of potentials, the anodic Tafel slope can be determined and then the value of B can be calculated by using Eq. (3).

However, using the abovementioned method to determine the value of B for steel bars in concrete is not an easy task since the scan rate for the experiment should be very low and in addition to being time consuming, the corrosion behavior could change considerably during the time of testing [11]. Therefore, in this paper another approach is used which can provide corrosion current density and the value of B rapidly. In this study, the potentiostatic transient technique is used to directly determine the corrosion current density of steel rebars. In this technique, a constant potential signal (usually ± 10 mV or ± 20 mV) is applied for a certain period of time, which is determined by the time for current to reach steady state, in the form of a square wave between the working electrode (steel bar in concrete) and reference electrode, and the response current is measured. Fig. 3 schematically shows the applied potential and current response during potentiostatic transient measurement.

When steel is polarized, the charge consumed from time $t=0$ to t can be written as follows:

$$q_{\text{total}} = \int_0^t Idt \tag{7}$$

where q_{total} is the consumed charge in coulomb, t is the time (s) and I is current (A).

Therefore, the area under the current–time curves ($S_a + S_c$ in Fig. 3) can be used to determine the consumed charge during the polarization process.

It is imperative to note that this is the total consumed charge in both the interfacial corrosion process and the double layer capacitance.[1] Therefore, the effect of capacitance should be considered in the calculations. The charge used by the double layer capacitance can be determined using Eq. (8):

$$q_{\text{dl}} = C_{\text{dl}} \times V \tag{8}$$

where C_{dl} is the double layer capacitance (F) and V is the potential (V). The value of the capacitance can be determined using electrochemical impedance spectroscopy or galvanostatic pulse technique [12], and as it is described in [12], dertmining the double layer capacitance is a

[1] When an electrode, in this case steel rebar, is in contact with the electrolyte solution, which in concrete is the pore solution, electrical charges accumulate on the surface and charge separation occurs at the interface of the electrode (steel) and the electrolyte (pore solution). This structure behaves essentially as a capacitor and is called double layer capacitance.

relatively easy task. By deducting q_{dl} from q_{total}, the consumed charged during the corrosion processes can be calculated.

$$q_{corr} = \Delta q_{total} - q_{dl} \tag{9}$$

q_{corr} represents both charges obtained from anodic polarization and cathodic polarization with considering the effect of double layer capacitance. The mass loss during the polarization time can then be calculated by applying the Faraday's law as following:

$$m = \frac{q_{corr} \times M}{n \times F} \tag{10}$$

where m (g) is the mass loss during the polarization time, M is the atomic weight of steel (~55.845 g/mol), n is the number of equivalent exchanged electrons (in this case considered 2), and F is Faraday's constant (96,500 C mol^{-1}). The amount of mass loss can be then determined per year and the penetration depth can be calculated as:

$$d = \frac{m_y}{\rho \times A} \times 10 \tag{11}$$

where d is the penetration depth (μm/year), m_y is the mass loss per year (g) and A is the corroding area (cm^2). For iron, $M = 55.845$ g/mol, $\rho = 7.875$ g/cm^3, and $n = 2$, therefore:

$$i_{corr}\left(A\,m^{-2}\right) = \frac{Corrosion\,rate\,(\mu m/year)}{0.116}. \tag{12}$$

Then, the value of B can be determined from the current density, using Eq. (2).

2. Materials

Nine concrete specimens, three with 0.3 mm transverse crack (perpendicular to the steel bar), three with 0.3 mm longitudinal crack (parallel to the steel bar) and three without a crack, with the geometry shown in Fig. 4a, were used. Plain carbon steel with the diameter of 10 mm was used in each specimen. One end of the rebar was tapped and a stainless steel screw was used for electrical connection. Both ends of the steel bar including the electric connection were epoxy coated. The coated length inside the concrete was equal to the cover depth which left the exposed length of 400 mm on the steel bars. Concrete mixture proportions are given in Table 1. After casting, specimens were wet cured for two days and then they were kept in the laboratory condition for 28 days before inducing the transverse cracks using three point bending. To cause longitudinal cracking (i.e. parallel to the steel rebar), a PMMA rod (polymethyl methacrylate), with the diameter of 10 mm, was positioned underneath the steel rebar and the samples were exposed to temperature variation from −32 to +32 °C, for three months. The thermal expansion coefficient of the PMMA rod is between 60 and 90×10^{-6} °C^{-1} [13], and that of cement paste is around 11–20×10^{-6} °C^{-1} [14]. The temperature variation was created cracks parallel to the steel rebar.

Exposure of all specimens to salt solution was started four months after casting. A ponding well, made of plexiglas sheets, was installed on top of each specimen and was filled with a 3 wt.% chloride (NaCl) solution and the specimens were alternately exposed to 2-week periods with solution then 2 weeks without solution. Measurements were performed during the second week of the wet period.

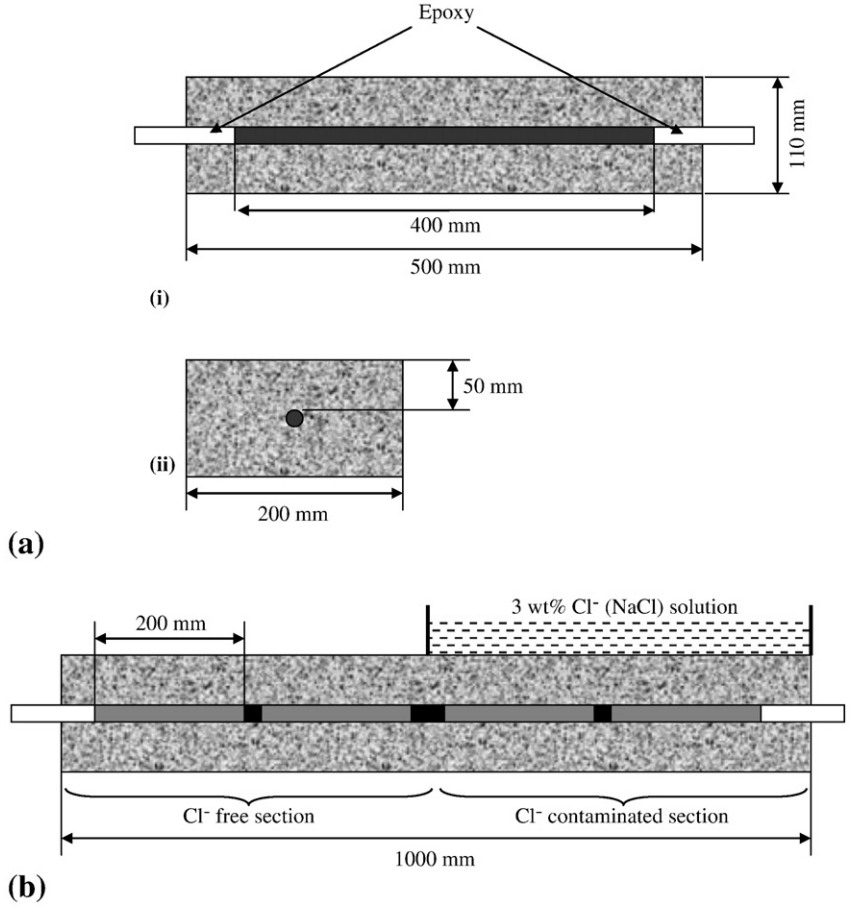

Fig. 4. Schematic plans of (a) a concrete specimen with one steel bar: (i) side view, (ii) end view and (b) a concrete specimen with segmented steel bars with the same end view as shown in (a)-ii.

Table 1
Concrete mixture proportions for making 1 m^3.

Component	
Type 10 portland cement (kg)	355
Fine aggregate (kg)	770
Coarse aggregate (20 mm) (kg)	1070
Water (liter)	160
Air entraining admixture (Eucon MRC)	40 ml/100 kg cement
Water to cement ratio	0.45

In addition to the aforementioned specimens, three beams with one pre-weighted segmented ($\Phi = 10$ mm) in each were cast as illustrated in Fig. 4b. These specimens were later autopsied and the amount of mass loss was calculated and compared to what was estimated using potentiostatic transient method and conventional LPR technique (using constant values of B for active and passive states). To separate and isolate the steel segments, a small plastic spacer was used between each segment. For electrical connection, copper wires were used and connected to each steel segment. The ends of the bars exposed to the atmosphere were coated with epoxy resin to define the exposed length of 200 mm of the bar. The concrete for each beam was cast in two parts: for one half was as given in Table 1 while the concrete for the second half had the same mixture proportions but with 2.5% chloride by weight of cement added to the mixing water as NaCl. Later in the process, a ponding well was installed on the Cl^- contaminated part of each beam and that section was alternately exposed to 2-week periods with 3 wt.% chloride (NaCl) solution then two weeks without solution to accelerate the corrosion on that side. The same curing regime which was explained above, was used for these specimens as well.

3. Experimental procedures

Corrosion activity of the steel bars in all samples was examined for 85 weeks. Half-cell potential of the rebars were monitored by measuring the potential of the steel bar against $Cu/Cu(SO_4)$ reference electrode and potentiostatic transient method and conventional LPR technique were used to measure the corrosion current density of the steel bars. For the potentiostatic transient test, ± 20 mV versus the E_{corr} was applied to the steel bars, for 150 s on each direction (total time = 300 s). It should be mentioned that the amount of mass loss could also be determined by applying just $+20$ or -20 mV versus E_{corr}. However, by using both anodic and cathodic polarization, both reactions are being considered and the results would be more realistic.

Polarization measurements in concrete include an ohmic potential drop through the concrete cover. This ohmic potential drop always occurs between the working electrode and the capillary tip of the reference electrode which affects the detected potential by the reference electrode, and consequently, usually causes underestimation of the corrosion current density. Therefore is important to consider the concreter resistance in all the calculations. The concrete resistance (shown in Fig. 5b) and double layer capacitance were also measured, using the galvanostatic pulse technique [12], by applying 100 μA for 60 s; and the effect of ohmic resistance and the double layer capacitance on the applied potential was compensated in all calculations. In order to perform corrosion measurement tests, a piece of stainless steel (200 mm × 100 mm) with a hole, with the diameter of 10 mm at the center, was placed on top of each sample during the measurement and used as the counter electrode. To facilitate the connection, a wet sponge was used between the counter electrode and the surface of the each specimen. Saturated Calomel Electrode

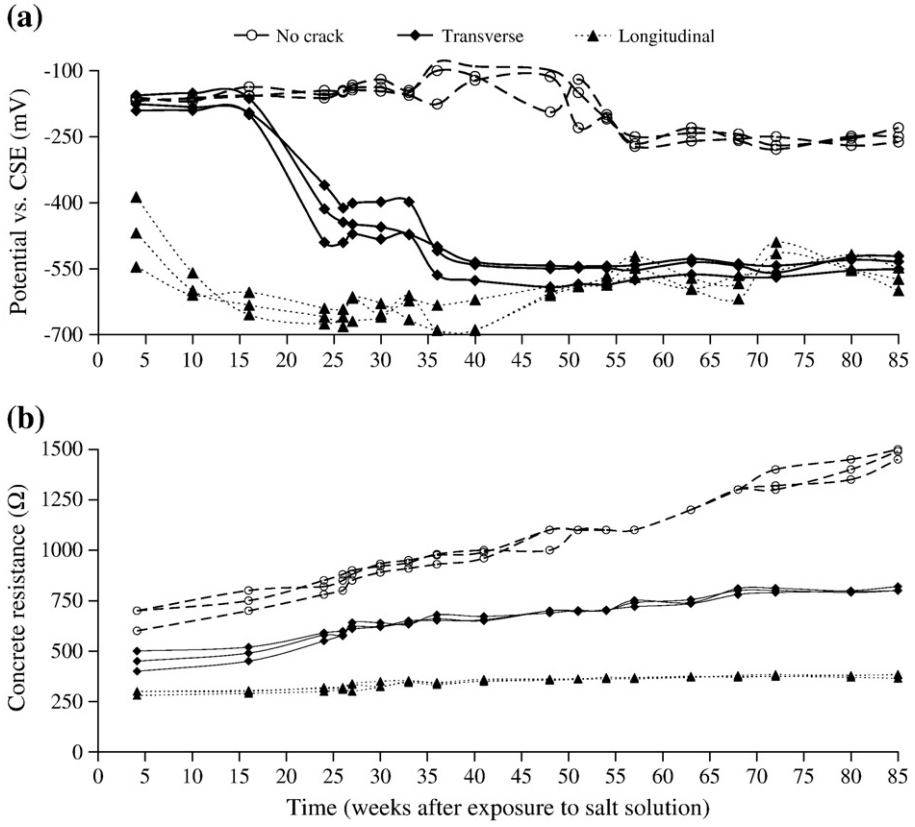

Fig. 5. (a) Corrosion potential (versus $Cu/Cu(SO_4)$ reference electrode) and (b) concrete resistance of the specimens with and without crack.

Table 2
Value of B, calculated for different specimens at different times by using (a) potentiodynamic polarization, and (b) potentiostatic transient method.

Specimen	B (mV)					
	Time (weeks after exposure to salt solution)					
	Week 20		Week 40		Week 80	
	a	b	a	b	a	b
Transverse crack	22.3	23.0	23.1	22.1	16.9	16.2
Longitudinal crack	16.0	15.5	15.0	14.5	14.0	13.4
No crack	73.2	72.9	73.3	73.0	75.8	76.5

(SCE) was placed at the center of the counter electrode and used as the reference electrode. To determine the corrosion current density, two approaches were used. First the current densities were calculated using $B = 26$ mV and 52 mV for cracked specimens (active state) and specimens with no crack (passive state), respectively. In addition, the area under the curve of current versus time was determined ($S_a + S_c$ in Fig. 3) and then the current density calculated based on the amount of mass loss during the period of the test.

To confirm the B values obtained from the potentiostatic transient method, B was also determined using anodic and cathodic polarization curves for each specimen at different ages. For this purpose, different scan rates from 0.05 to 0.1 mV s^{-1}, based on the corrosion condition of the steel bar in each specimen, were calculated and used [12]. The scan was started at −100 mV and increased to +100 mV versus the corrosion potential (E_{corr}).

To confirm that there was no active corrosion on the steel bar in the specimens without a crack, one of those samples was autopsied after 85 weeks of exposure to salt solution and no corrosion product was found at the surface of the steel rebar. In addition, the chloride content at the steel imprint and 10 mm above the steel imprint was analyzed. For this purpose, a cylindrical-radius carbide drill bit was used to pulverize the concrete adjacent to the steel surface. The ASTM C1152 [15] standard was used to determine acid-soluble chlorides

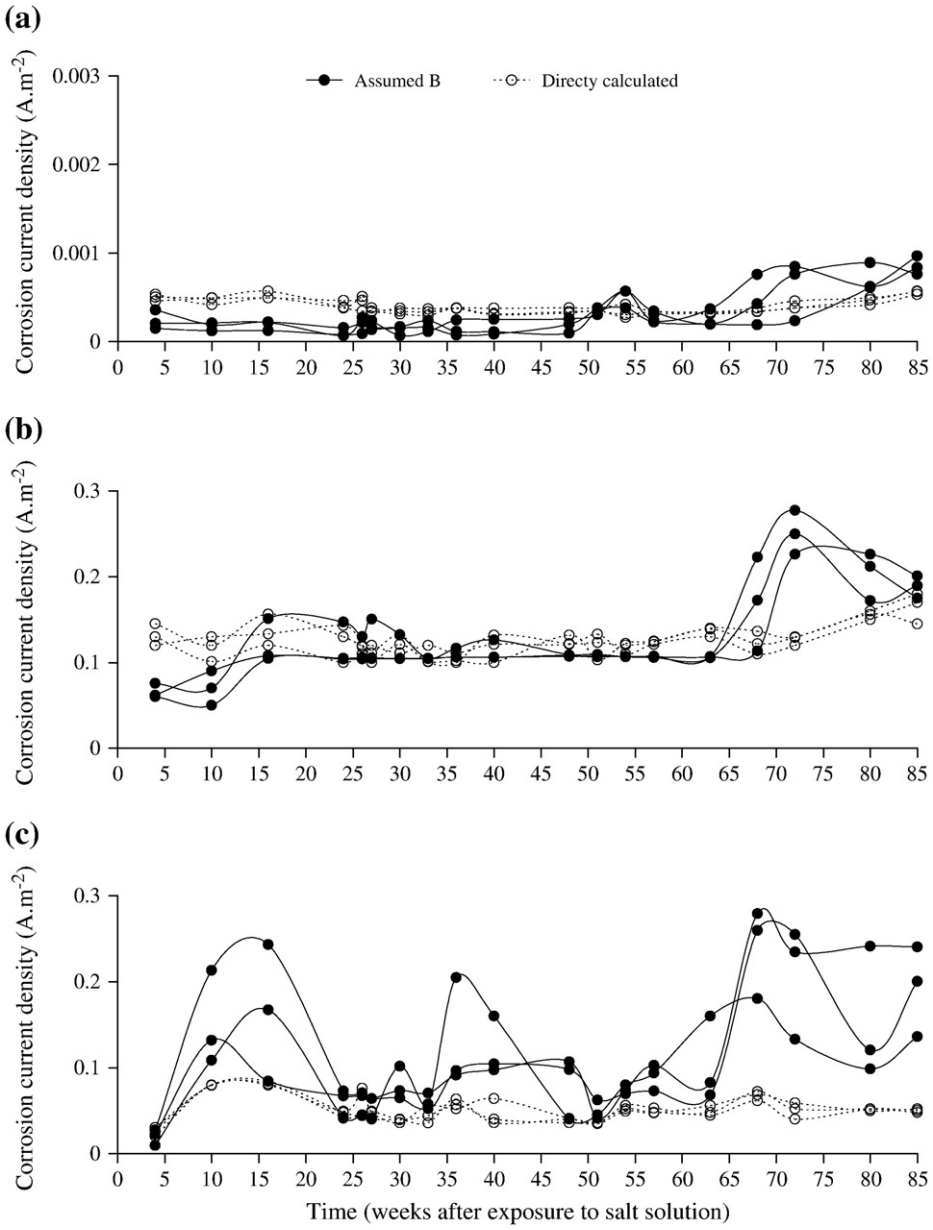

Fig. 6. Corrosion current densities directly calculated from current–time curves and calculated using the assumed values of B: (a) specimens without crack, (b) specimens with transverse crack, and (c) specimens with longitudinal cracks.

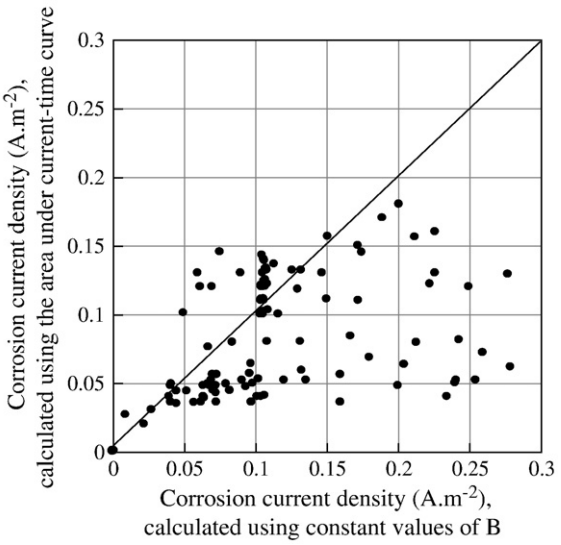

Fig. 7. Plot of corrosion current densities of all samples directly calculated from the area under the current–time curve versus calculated using assumed values of *B*.

which consists of both free and chemically bound chlorides in the cement paste. No trace of chloride was found in the aforementioned locations. One of each cracked specimens was also autopsied at the end of the experiment to examine the extension of the corroded area. Corrosion was observed on the surface of the steel bar in specimens with transverse crack, adjacent to the crack location, within a region of about 10 mm from each side of the crack location. In the specimen with longitudinal crack, corrosion was observed on approximately 25% of the top surface of the bar. Therefore, in the calculations, 400 mm and 20 mm of the length of the steel bar were used to calculate the corroded surface area in the specimens without a crack and with transverse crack, respectively. For the specimens with longitudinal crack, a quarter of the surface area of the steel bar with the length of 400 mm was used for the calculations.

The corrosion current densities of the segmented steel bars (Fig. 4b) were also determined using both potentiostatic transient method and the conventional LPR technique. The same setup and procedures was used to perform the tests as explained above. At the end of the measuring period, all beams were autopsied and the corrosion products on each steel segment were removed according to ASTM G1 [16] standard procedure. The steel segments were immersed in Clark solution (1000 ml hydrochloric acid solution (HCl, with specific gravity = 1.19) + 20 g antimony trioxide (Sb_2O_3) + 50 g stannous chloride ($SnCl_2$)) until the corrosion products were entirely removed. After removing the corrosion products, the corroded area on each segment was estimated and used to calculate the corrosion current density. By using the area under the corrosion current density versus time curves, the cumulative mass loss was calculated and compared to the actual mass loss.

4. Results and discussion

As mentioned before, to confirm the results of *B* obtained from the area under the current–time curve, *B* was also calculated at different times for one of each type of specimens with no segmented rebars, by determining β_a and β_c from anodic and cathodic potentiodynamic polarization curves, and then using Eq. (3). Results of such comparison are given in Table 2. As can be seen, the values are very similar to each other with less than 5% difference. This suggests that the proposed approach is a valid method for the determination of corrosion current density and consequently the value of *B*.

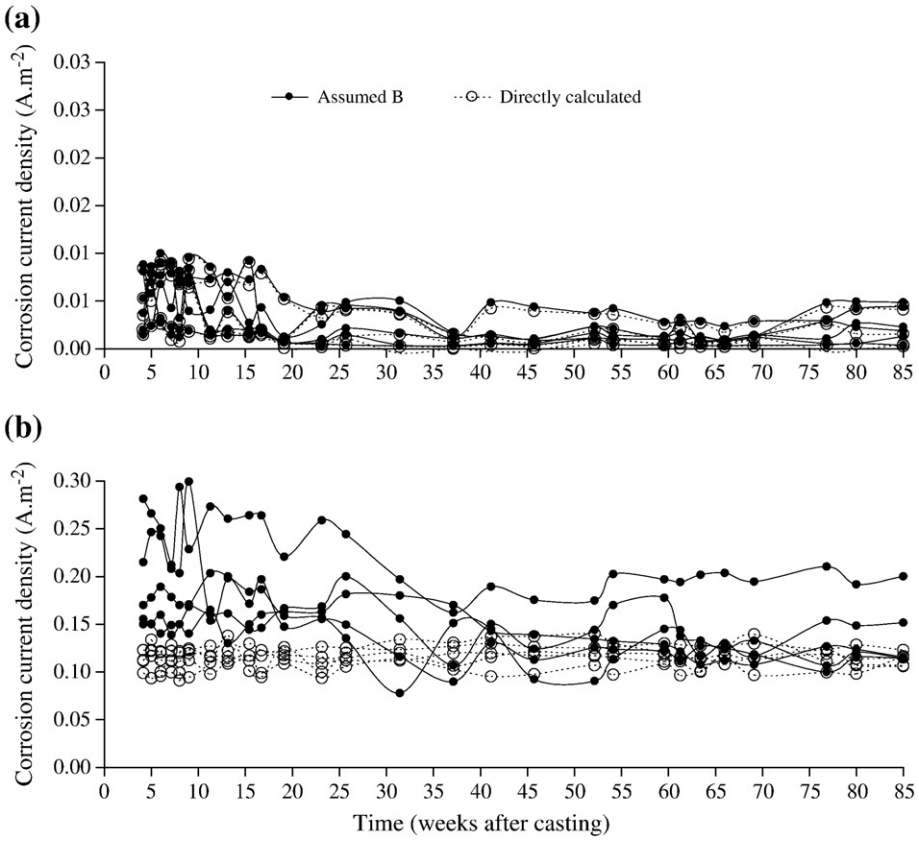

Fig. 8. Corrosion current densities directly calculated from current–time curves and calculated using the assumed values of *B* in concrete with segmented steel bars in: (a) chloride free section and (b) chloride contaminated section.

The results of the corrosion potential are shown in Fig. 5. As can be seen the half-cell potential of steel bars in the cracked specimens shows more than 90% probability of active corrosion while the half-cell potential of the steel bars in specimens with no crack stays in the region corresponding to less than 10% probability of corrosion [17]. It should be mentioned that the half-cell potential of the samples with transverse crack indicates low probability of corrosion up to 15 weeks after exposure to the chloride solution while the corrosion current densities (Fig. 6) showed the opposite results. Small anode to cathode ratio in specimens with transverse cracks, up to 15 weeks, could be one of the reasons of such behavior [18]. The limitations of half-cell potential technique are discussed elsewhere with more detail [11].

Corrosion current densities directly calculated using the area under the current–time curve were compared to those calculated using constant values for B (26 and 54 mV for active and passive states, respectively) and the results are show in Fig. 6. It should be noted that the ordinate scale for the specimens without a crack (Fig. 6a) is two orders of magnitude smaller than that for cracked specimens. As can be seen, when the corrosion is more localized (transverse crack), or when the steel is in passive state, the effect of B on the calculation of the corrosion current density is not considerable, and using 26 mV does not change the results significantly. However, by increasing the corroded area and having less localized and more uniform corrosion (i.e. longitudinally cracked specimens, Fig. 6c), the corrosion densities determined using constant values of B divert from the directly calculated ones. In addition, current densities of specimens with longitudinal cracks show more fluctuation when the constant value of B (26 mV) is used, while directly calculated corrosion densities show less inconsistency. This is more reasonable since all the specimens were kept in the laboratory condition during the whole experiment period. The corrosion densities of one of each specimen were also measured by potentiodynamic LPR at different times, and the results were similar to those measured directly from the area under current–time curve obtained from the potentiostatic transient technique.

To show the effect of B on the corrosion density more clearly, the corrosion current densities of all specimens without segmented bars determined directly from the current–time curves are plotted versus those using the assumed values of B which is shown in Fig. 7. It can be seen that it is difficult to find a linear relationship between two corrosion current densities and the discrepancies between the values are greater when the corrosion rate is higher.

Results of corrosion measurement of steel segments in specimens with segmented bars are shown in Fig. 8. It should be noted that the ordinate scale for the steel in contaminated section is an order of magnitude greater than that for the steel in chloride free section. As can be seen, like the other sets of specimens (Fig. 6), by having more corrosion in the system (chloride contaminated section) the corrosion current densities determined by potentiostatic transient method show less fluctuation. All of these specimens were autopsied at the end of the experiment and mass loss was determined and compared to what was calculated from potentiostatic transient method and conventional LPR technique (using constant values of B). Fig. 9a and b shows the mass loss of all segments determined using gravimetry technique versus that calculated using potentiostatic transient method and conventional LPR, respectively. It is clear that mass loss values calculated by the potentiostatic transient method are very close to what was determined by the gravimetry technique. In addition, calculations performed using the constant values of B (Fig. 9b) show more discrepancies in chloride contaminated section compared to the actual mass loss determined by the gravimetry. This is in agreement with what was seen for the other sets of specimens (specimens with no segmented bars) and confirms that the discrepancies between the values are greater when the corrosion rate is higher.

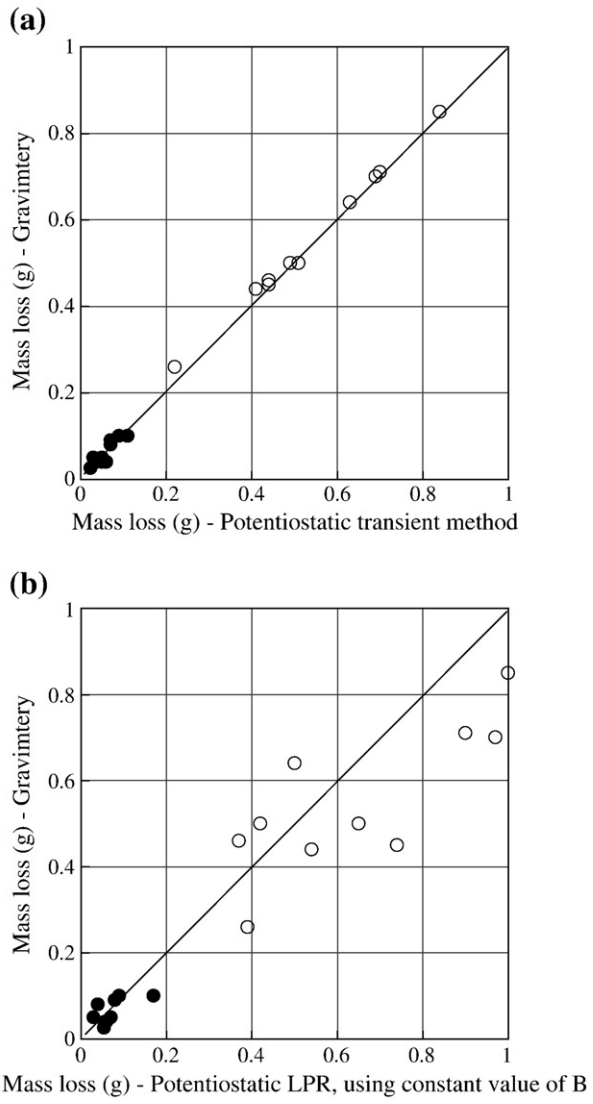

Fig. 9. Plots of mass loss of all steel segments (○—Cl^- contaminated and ●—Cl^- free) determined by gravimetry versus (a) mass loss calculated from the potentiostatic transient method and (b) mass loss calculated using assumed values of B.

The results in Table 2, show that the average value of the B constant for passive (specimens without crack) and active (cracked specimens) states of corrosion of steel bars in concrete were ~75 mV and ~15 mV, respectively. However, since B is a function of anodic and cathodic reactions at the time of measurement, the aforementioned values might be only valid for the specimens used in this study. Therefore, measuring the B value for each case or using direct calculation of corrosion current density is recommended.

5. Conclusion

1. Potentiostatic transient technique was used as a simple and relatively fast technique to calculate the corrosion current density of steel rebars without knowing the value of B.
2. By having more active corrosion, the corrosion rates determined using the conventional LPR show more fluctuations and illustrate more discrepancies compared to the actual corrosion rate (mass loss) while the values obtained from the potentiostatic transient method show less fluctuations and are very close to the actual values.
3. The effect of ohmic resistance and double layer capacitance needs to be considered in the calculations, using potentiostatic transient technique.

4. Results from 85 weeks of corrosion measurements of the steel in three different concrete specimens show that the Stern–Geary constant (B) was ~15 mV for active corrosion and ~75 mV for passive corrosion. However, due to variation of B by time and environment, measurement of B for each specimen at the time of experiment or direct calculation of corrosion current density is recommended.

Acknowledgement

The author would like to thank Professor Carolyn Hansson for her extensive contributions in this study.

References

[1] M. Stern, A.L. Geary, Electrochemical polarisation: I. A theoretical analysis of the shape of polarisation curves, J. Electrochem. Soc. 104 (1) (1957) 56–63.
[2] C. Andrade, J.A. González, Quantitative measurements of corrosion rate of reinforcing steels embedded in concrete using polarization resistance measurements, Werkst. Korros. 29 (1978) 515–519.
[3] C. Andrade, A. Marcias, S. Feliu, M.L. Escudero, J.A. Gonzalez, Quantitative measurement of the corrosion rate using a small counter electrode in the boundary of passive and corroded zones of a long concrete beam, in: N.S. Berke, V. Chaker, D. Whiting (Eds.), Corrosion Rates of Steel in Concrete, ASTM STP 1065, ASTM, Philadelphia, PA, 1990.
[4] U. Bertocci, Impedance spectroscopy for the evaluation of corrosion inhibitors in highway deicers, FHWA-RD-96-178, Research and Development, Turner-Fairbank Highway Research Center: Georgetown Pike, 1997.
[5] N.G. Thompson, K.M. Lawson, An electrochemical method for detecting ongoing corrosion of steel in a concrete structure with CP applied, Strategic Highway Research Program, National Research Council, Washington, DC, 1991.
[6] G. Song, Theoretical analysis of the measurement of polarisation resistance in reinforced concrete, Cem. Concr. Compos. 22 (2000) 407–415.
[7] C. Alonso, C. Andrade, M. Izquierdo, X.R. Novoa, M.C. Perez, Effect of protective oxide scales in the macrogalvanic behaviour of concrete reinforcements, Corros. Sci. 40 (8) (1998) 1379–1389.
[8] C.E. Locke, A. Siman, Electrochemistry of reinforcing steel in salt contaminated concrete, Corrosion of Reinforcing Steel in Concrete, ASTM STP713, Philadelphia, 1978.
[9] D.A. Jones, N.D. Greene, Electrochemical measurement of low corrosion rates, Corrosion 22 (1966) 198–204.
[10] D.A. Jones, Principles and Prevention of Corrosion2nd ed, Prentice Hall, 1995.
[11] A. Poursaee, C.M. Hansson, Potential pitfalls in assessing chloride-induced corrosion of steel in concrete, Cem. Concr. Res. 39 (5) (2009) 391–400.
[12] A. Poursaee, Determining the appropriate scan rate to perform cyclic polarization test on the steel bars in concrete, Electrochim. Acta 55 (3) (2010) 1200–1206.
[13] D.R. Lide, CRC Handbook of Chemistry and Physics, CRC Press, New York, NY, 1999.
[14] A.M. Neville, Properties of Concrete4rd ed., Longman Scientific & Technical, New York, N. Y., 1995
[15] ASTM C1152, Standard Test Method for Acid-soluble Chloride in Mortar and Concrete, ASTM, 1997.
[16] ASTM, G1-90: Standard Practice for Preparing, Cleaning, and Evaluating Corrosion Test Specimens, ASTM, 1999.
[17] ASTM, C876-09: Standard Test Method for Half-cell Potentials of Uncoated Reinforcing Steel in Concrete, 2009, pp. 446–451.
[18] M. Pour-Ghaz, O.B. Isgor, P. Ghods, Quantitative interpretation of half-cell potential measurements in concrete structures, J. Mater. Civ. Eng. (2009) 467–475 September.